# TEXTURE-SPACE SEGMENTATION AND MULTI-RESOLUTION MAPPING FOR FORESTRY APPLICATIONS

*Matthew Hill, Yuan-Chi Chang, Vijay Iyengar, Chung-Sheng Li*

IBM T.J. Watson Research Center
P.O. Box 704
Yorktown Heights, NY 10598

## ABSTRACT

Forestry management requires careful and intensive planning efforts to ensure optimal yield, ecological stability, and regulatory compliance. In this paper, we describe a method of identifying wetlands and producing maps of their extent from commonly available, remotely-sensed imagery. This method provides a large labor savings over both field inspections and manual photo inspections. The enhanced accuracy translates into better timber harvest planning and better conservation of the wetlands.

## 1. INTRODUCTION

Wetlands are defined as "lands transitional between terrestrial and aquatic systems where the water table is usually at or near the surface or the land is covered by shallow water."[1] There are several industries concerned with studying wetlands. From the point of view of a timber company, wetlands represent a significant challenge in harvest planning. Wetlands do not produce much timber, since typically harvested trees prefer to grow in drier soil. Additionally, it is difficult to operate harvesting equipment in wetlands.

Wetlands support a large number of both species that cannot survive anywhere else. For this reason, federal regulations such as the Clean Water Act (33 United States Code Part 1344), as well as varying state laws, disallow many activities in wetlands, including logging.

However, wetlands are not only an interest of those in the forestry industry. Any party to a real estate transaction has a pecuniary interest in determining if any parts of the property are subject to wetland regulations. To know exactly how much and which parts of the property is wetland is even more valuable.

We propose a two-step method of wetland mapping using remotely sensed imagery. Rather than start anew from the raw data, we choose to leverage an existing technology from the forestry industry. Weyerhaeuser Corporation currently generates maps of wetland areas from Landsat-TM imagery that represent their best automatically generated estimate of the wetlands. We use these maps, which are relatively low-resolution, as a source of information complementary to relatively high-resolution aerial photography which we process with respect to texture. When combined, our segmented texture map and the previous estimate generate a highly accurate and precise wetland map.

The authors would like to thank Zhenkui Ma and the Weyerhaeuser Corporation for providing imagery and their expertise on wetlands.

## 2. CURRENT WETLAND MAPPING

The region we studied was a six by six mile township in Washington state. Our main source of data was an aerial photo which has a resolution of 2 meters per pixel. Figure 1 shows a well-known wetland area in detail for which we will summarize our results. Three salient areas have been indicated by hand. The challenge is to delineate the boundaries between these areas on a pixel-by-pixel basis. This is made difficult by the fact that although some boundaries are quite obvious – such as that between the conifer and clear cut areas – other boundaries are non-existent, and must be inferred from the presence of nearby boundaries.

The current state of the art, as used by Weyerhaeuser, is described by Ma et al.[2] In brief, Landsat TM imagery is used by an expert operator to select some examples of wetland areas to form a training set. As an alternative to manual selection, the training set could, in large part, be derived from known wetland areas in the National Wetlands Inventory database, provided by the federal government. The NWI database, in practice, turns out to be a conservative estimate of wetland areas, meaning that not all wetlands are marked, but areas that are marked do actually represent wetlands. In a process of iterative refinement, a Gaussian maximum-likelihood based classifier is used to classify each Landsat pixel as wetland or non-wetland. The Landsat imagery used is at a resolution of 28.5 meters per pixel, and includes multiple bands. Among these are both infrared and visible light bands. The infra-red band carries useful information about the presence of water in the area. In

each iteration, the operator may modify the training set used by the classifier, adding examples which were not captured previously.

This process results in a map generated at a resolution of 28.5 meters per pixel, as show in figure 5. As can be seen, the map bears a resemblance to the wetland area shown in figure 1, however, its low resolution precludes it from accurately estimating the area of the wetlands. This classification can be thought of as an accurate "detector" of wetlands. That is, over the entire 36 square miles, this classifier will produce "blobs" similar to figure 5, the location of which indicates wetlands in the vicinity.

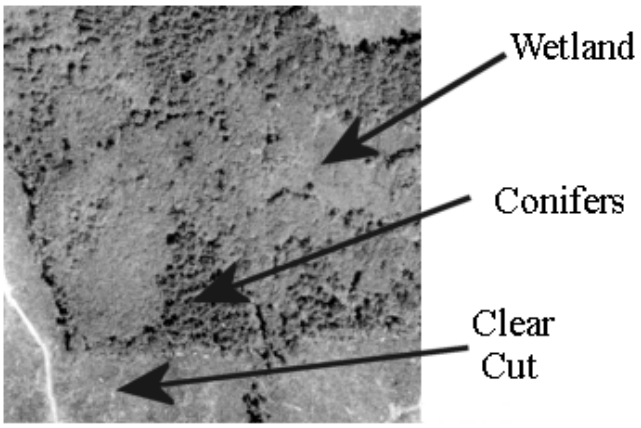


**Fig. 1**. Detailed area of study. Note that the wetlands, roughly in the central area of the figure, are interspersed with trees. There is also a break in the stand of conifers, towards the lower left, where the wetlands are contiguous with the previously clear cut area.

## 3. HIGH RESOLUTION WETLAND MAPPING

There are two main challenges to higher resolution wetland mapping. First, the borders which are apparent to the eye immediately in the high resolution aerial photography are not well traced in low resolution maps like figure 5. There is obvious "wandering" from the true border. This stems from the fact that in the 28.5 m per pixel Landsat imagery, the fine border of tree lines is not well-defined, even to the expert eye. Our solution to this problem lies in generating a high-resolution map from the aerial photos and is described in section 3.1.

The second issue is that areas that appear contiguous and homogeneous in the visible-spectrum aerial photos may actually be heterogeneous. However, we have observed that the maps generated from Landsat imagery (based partially on the infra-red bands) do discriminate between these areas. We propose, and have implemented, the method described in section 3.2 for combining the high- and low-resolution maps to generate our final, high resolution, high accuracy map.

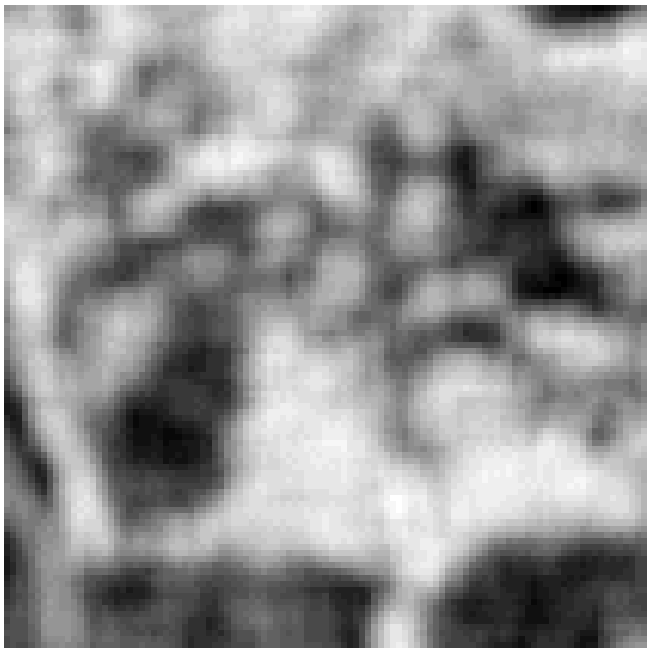

**Fig. 2**. Mean Entropy feature map for the area shown in figure 1. Lighter shades mean greater entropy.

### 3.1. Texture Segmentation

An early observation we made was that the aerial photo, considered as a luminance image, was uncorrelated with the locations of wetlands. The image had to be transformed into the texture domain to proceed with a meaningful segmentation. Texture features have been used in wetland applications before, as in Yamagata and Yasuoka, who applied them to ERS-1 and JERS-1 imagery.[3] They used the texture features as input to a classifier. We use the texture features as an input to a segmentation algorithm. We adopted this approach after we attempted several classification schemes, and found the results unsatisfactory. This was due to the fact that there are multiple classes of wetlands present in the imagery. Similarly, Yamagata and Yasuoka note that out of more than six classes of wetlands, only two (bog and water inundated) were distinguishable in the JERS-1 imagery using their classifier.

Our image segmentation algorithm relies on the local values of the texture feature being processed. It does not require specific classes to be prepared ahead of time as training sets. Any sufficient change in the feature value will result in a segment being demarcated. We began by creating a texture vector based on the features described in Gu et al.[4] Empirical testing showed that the mean entropy feature provided the best segmentation, and the other elements of the

vector were discarded. Mean entropy is calculated as the average of:

$$-\sum_{i=0}^{G} \frac{f_{\delta,\theta}(i)}{L} \log\left(\frac{f_{\delta,\theta}(i)}{L}\right)$$

$f_{\delta,\theta}(i)$ represents a probability density function for distance $\delta$ and angle $\theta$ for a point $(n, m)$ in the image. This is the probability that the difference between the pixel value at location $(n, m)$ and the pixel at $(n, m) + (\delta, \theta)$ is equal to $i$. $L$ represents the sample size.

The value of the mean entropy function for the image area we are considering is shown in figure 2.

We then segment the entropy map shown in figure 2 using a standard edge detection algorithm into a set of regions. As shown in figure 3, this results in a meaningful segmentation: the conifer area is clearly demarcated along all of its boundaries, and small clumps of trees in the middle of the wetland area have also been isolated.

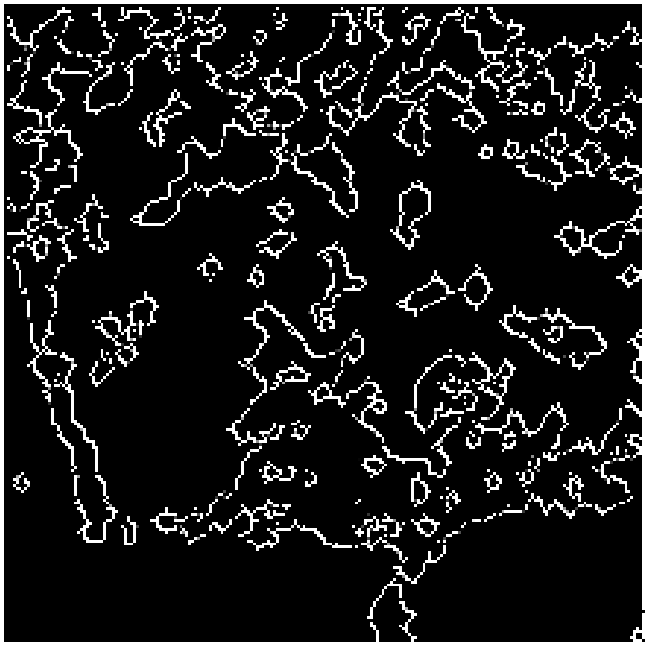

**Fig. 3**. Boundaries resulting from segmenting the texture feature map.

Figure 4 shows these boundaries superimposed upon the aerial photo. The boundaries closely follow the changes in texture in the image. However, the boundaries sometimes fail to divide regions of wetland from clear cut regions. The lower left corner of figure 4 is an example of this. To "seal off" these boundaries, we combine the previous, low resolution map with our new high-resolution boundaries.

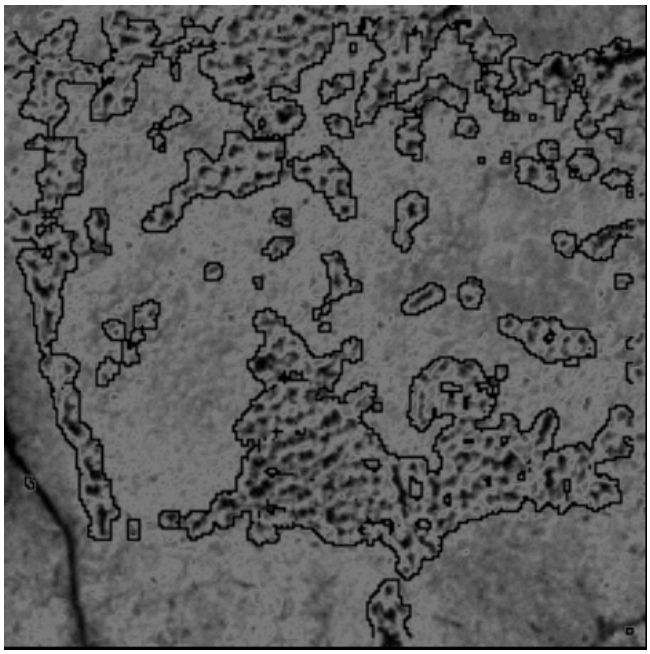

**Fig. 4**. Boundaries from texture segmentation overlaid on aerial photography. (Solarized for better contrast.)

### 3.2. Merging Multi-Resolution Estimates

To provide the best estimate of the wetland boundaries, we merge the low-resolution (figure 5) and high resolution (figure 3) maps. We begin with the observation that the Landsat-generated map is a good indicator of the size and general shape of a wetland region. The aerial photo segmentation provides meaningful boundaries, but gives no semantic indication of which segments are wetlands.

The first step is to coregister the two maps so that they represent the same area at the same, high resolution scale. We apply a binary morphology operator to dilate the low-resolution map. This serves to unite isolated blocks in this map with nearby, larger regions. The low-resolution map is only providing the rough location of wetlands. The dilation does not serve to simply dilate the final borders because the map is combined with the high-resolution map later.

Next, we perform a connected components analysis of each map. This results in two new maps in which each region of 8-connected pixels is labelled with an integer. Say there are $x$ components in the low-resolution map and $y$ components in the high-resolution map. Let $L(p, q)$ and $H(p, q)$ represent the integer label of image point $(p, q)$ in the low and high-resolution maps, respectively.

We then construct a coincidence matrix $C$ of size $x \times y$. $C(m, n)$ contains the number of pixels in component $m$ in the low-resolution map that are in component $n$ in the high resolution map. The background component of the low-resolution map is omitted from this matrix. Then, for each

component $m$ in the low-resolution map, we find the component $n$ from the high-resolution map with the most shared pixels. This corresponds to computing a vector $M$ of length $x$ where:

$$M(i) = \arg\max_{n} \{C(i, n)\}$$

This serves to match up low-res and high-res components. The final map is constructed at high resolution as follows. For each pixel position $(p, q)$, if $H(p, q) = M(L(p, q))$ then we denote $(p, q)$ as wetland in the output image.

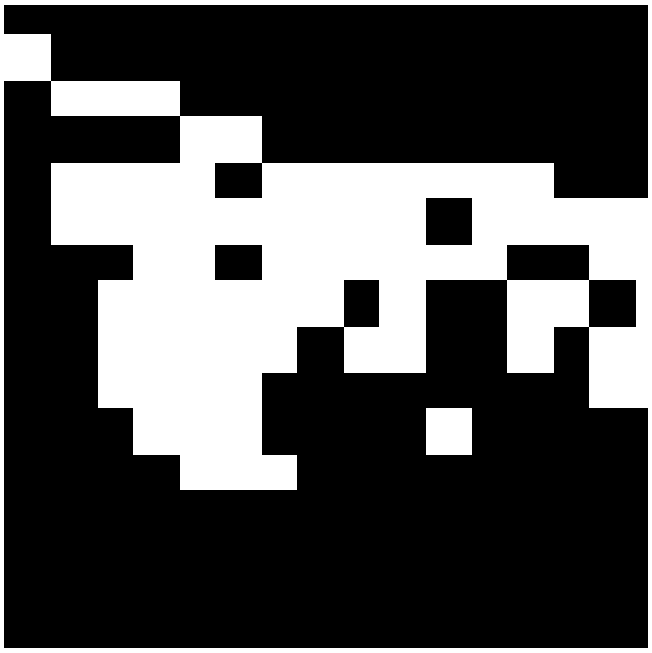

**Fig. 5**. The results of classifying the Landsat imagery. White represents wetlands.

This method limits the extent of a wetland border to the dilated components from the low-resolution map. However, it simultaneously allows high-resolution borders to take precedence. In other words, the extent of a "leak" from a high-resolution region is limited by the low resolution map estimate. The final result mask is shown in figure 6.

## 4. CONCLUSION

Contrasting figure 6 and figure 5 it is immediately apparent that the results shown here represent a significant improvement in the precision of wetlands mapping. The resolution has been improved by a factor of over 14 times. Field trips to this well-known wetland area have confirmed that the boundaries lie as predicted, establishing the accuracy of the method. The results for the rest of the township are currently under evaluation in the field.

**Fig. 6**. Final results showing high-resolution wetlands.

This represents a novel method and advance in the state of the art for mapping wetland boundaries. Merging two estimates, one robust in accuracy, the other robust in precision, forms a more useful map that can be used to generate higher harvest yields and conserve precious natural resources.

## 5. REFERENCES


[1] L.M. Cowardin, V. Carter, F.C. Golet, and E.T. LaRoe, *Classification of Wetlands and Deepwater Habitats of the United States*, US Fish and Wildlife Service FWS/OBS-79/31, 1979.

[2] Zhenkui Ma, Melissa M. Hart, and Roland L. Redmond, "Mapping vegetation across large geographic areas: Integration of remote sensing and gis to classify multisource data," *Photogrammetric Engineering and Remote Sensing*, vol. 67, no. 2, 2001, to appear.

[3] Y. Yamagata and Y. Yasuoka, "Classification of wetland vegetation by texture analysis methods using ers-1 and jers-1 images," in *Better Understanding of Earth Environment*. International Geoscience and Remote Sensing Symposium, 1993.

[4] Z.Q. Gu, C.N. Duncan, E. Renshaw, M.A. Mugglestone, C.F.N. Cowan, and P.M. Grant, "Comparison of techniques for measuring cloud texture in remotely sensed satellite meteorological image data," in *IEEE Proceedings - Radar and Signal Processing*, 1989, vol. 136, pp. 236–248.